

In-situ microcalorimetry study on thermodynamic functions of Cu₂O nanocubes

Zijun He¹, Huanfeng Tang¹, Zaiyin Huang² ✉

¹Department of Chemistry and Chemical Engineering, Guangxi University for Nationalities, Nanning 530006, People's Republic of China

²Key Laboratory of Forest Chemistry and Engineering, Key Laboratory of Guangxi Colleges and Universities for Food Safety and Pharmaceutical Analytical Chemistry, Nanning 530006, People's Republic of China

✉ E-mail: huangzaiyin@163.com

Published in Micro & Nano Letters; Received on 22nd April 2019; Revised on 1st August 2019; Accepted on 28th August 2019

Four different sizes of cuprous oxides (Cu₂O) nanocubes in the range of 40–120 nm were synthesised by liquid phase reduction method. The morphology, size, and structure of synthesised Cu₂O nanocubes were characterised by scanning electron microscopy, X-ray diffraction, and X-ray photoelectron spectroscopy. In-situ microcalorimetry was used to calculate the conventional and surface thermodynamic functions of Cu₂O nanocubes by combining thermodynamic principles and transition state theory. The effect of particle size on conventional thermodynamic functions and surface thermodynamic functions were investigated and analysed, whose results were supported by the established thermodynamic models. Results showed that both the standard molar enthalpy of formation and the standard molar entropy of formation were increased with decreasing particle size, while the standard molar Gibbs energy of formation decreased. Also, the molar surface Gibbs energy, molar surface enthalpy, and molar surface entropy grew with the reduction of particle size, which correlated well with the models. Such a property is of scientific significance for enriching and developing disciplines such as surface physics and surface thermodynamics.

1. Introduction: Owing to unique surface and electronic structures, nanomaterials present specific surface physicochemical effects which are different from those of bulk materials [1]. These effects affect multiphase reactions of nanoparticles, including thermodynamics [2], dynamics [3] electrochemistry, [4] biological and antibacterial roles, [5] catalytic roles, [6] and sensing functions [7]. As a kind of p-type semiconductor catalyst with a bandgap in the range of 2.0–2.2 eV, cuprous oxides (Cu₂O) are characterised by their abundance, low price, and high adsorption coefficient. Therefore, they are considered as a candidate material to be used in solar power generation, lithium batteries, and photocatalytic hydrogen production [8]. Thermodynamic functions including Gibbs energy, enthalpy, entropy, and heat capacity are intrinsic characteristics for generating structure-function relationships between surface structure of nanomaterials and catalytic. Reducing the particle size to nanoscale can significantly increase the surface energy, which helps enhancing the reactivity [9]. Therefore, exploring the particle size effect on thermodynamic functions is conducive to understanding the essence of nanochemical reactions.

In 2016, Freakley [10] reported that the high catalytic activity was closely related to the PdSn catalyst particle size in H₂O₂ production in the journal *Science*. Recently, Jamshidian [11] has discovered, by continuum theory, that the surface energies of flaky, and spherical, nanoparticles decrease with the decrease of their particle sizes. Moreover, they verified this conclusion through density functional theory (DFT). By combining atom–atom pair potential theory with experimental results, Range [12] found that when the particle size $d > 100$ nm, the effect of surface energy on lattice energy was <2%; while $d < 20$ nm, this influence increased with the reduction of the particle size. Although the above studies provide a theoretical basis for the determination of surface energy, surface energy is generally calculated by ideal models, such as DFT, atomic arrangement, or atom–atom pair potential theory. There are a large number of atomic ladders and unsaturated bonds on actual surfaces of nanomaterials that are thermodynamically unstable. Therefore, developing a universal experimental method to obtain surface energy is currently a key problem to be solved in the surface science of nanomaterials.

In-situ microcalorimetry, [13–15] with its high precision and sensitivity is an effective experimental method for real-time on-line, monitoring of thermodynamic information in the changes of reaction systems. By combining the thermo-chemical cycles, thermodynamic principles, and the transition state theory of thermodynamics, the conventional and surface thermodynamic functions of nanoparticles can be acquired by this method. Therefore, it is acceptable to use microcalorimetry in the determination of surface energy verified by our previous work [15–17]. In this work, in-situ microcalorimetry was used to acquire the thermodynamic functions in the reaction process of Cu₂O with HNO₃. The conventional and surface thermodynamic functions of Cu₂O nanocubes were calculated by combining the thermochemical cycles and the basic theory of thermodynamics, and the effect of particle size on them have been discussed.

2. Methodology: According to the Gao [18] the equation of irreversible chemical reactions at constant temperature and constant pressure is

$$\ln \left[\frac{1}{H_{\infty}} \cdot \frac{dH_i}{dt} \right] = \ln k + n \ln \left[1 - \frac{H_i}{H_{\infty}} \right] \quad (1)$$

where H_{∞} represents the enthalpy change over the whole reaction process, H_i denotes the enthalpy change at time t , dH_i/dt denotes the rate of enthalpy change, k and n represent the reaction rate constant and the reaction order, respectively. By carrying out a least-squares regression on (1), the reaction rate constant k of the bulk and nano-Cu₂O in HNO₃ can be acquired. The relationships between the conventional thermodynamic functions of the bulk and nano-Cu₂O are:

$$\Delta G_m^{\theta} = \Delta_f G_m^{\theta}(\text{nano}) - \Delta_f G_m^{\theta}(\text{bulk}) = \Delta_r G_m^{\theta}(\text{bulk}) - \Delta_r G_m^{\theta}(\text{nano}) \quad (2)$$

$$\Delta H_m^{\theta} = \Delta_f H_m^{\theta}(\text{nano}) - \Delta_f H_m^{\theta}(\text{bulk}) = \Delta_r H_m^{\theta}(\text{bulk}) - \Delta_r H_m^{\theta}(\text{nano}) \quad (3)$$

$$\Delta S_m^{\theta} = \Delta_f S_m^{\theta}(\text{nano}) - \Delta_f S_m^{\theta}(\text{bulk}) = \Delta_r S_m^{\theta}(\text{bulk}) - \Delta_r S_m^{\theta}(\text{nano}) \quad (4)$$

where $\Delta_f G_m^\theta$, $\Delta_f H_m^\theta$, $\Delta_f S_m^\theta$ represent the standard molar enthalpy of formation, standard molar Gibbs energy of formation, and standard molar entropy of Cu_2O , respectively. $\Delta_r G_m^\theta$, $\Delta_r H_m^\theta$, $\Delta_r S_m^\theta$ delegate the standard molar enthalpy of reaction, standard molar Gibbs energy of reaction, and standard molar entropy of reaction of Cu_2O reaction system, respectively.

The relationship between the Gibbs energy of the reaction systems of nano- Cu_2O and that of bulk Cu_2O is obtained as follows:

$$\Delta_r G_{m(\text{nano})}^\theta - \Delta_r G_{m(\text{bulk})}^\theta = \Delta_r^\ddagger G_{m(\text{bulk})}^\theta - \Delta_r^\ddagger G_{m(\text{nano})}^\theta \quad (5)$$

According to the transition state theory

$$k = K \exp(-\Delta_r^\ddagger G_m^\theta / RT),$$

where K is a constant, proposed by Fu [19] and (2). The relationship between the reaction rate constant and the molar Gibbs energy of reaction can be acquired as

$$\Delta_r G_{m(\text{nano})}^\theta - \Delta_r G_{m(\text{bulk})}^\theta = RT(\ln k_{\text{nano}} - \ln k_{\text{bulk}}) \quad (6)$$

By combining (2) and (6), the standard molar Gibbs energy of formation of nano- Cu_2O is

$$\Delta_f G_{m(\text{nano})}^\theta = \Delta_f G_{m(\text{bulk})}^\theta - RT(\ln k_{\text{nano}} - \ln k_{\text{bulk}}) \quad (7)$$

In accordance with the formula $\Delta_r G_m^\theta = \Delta_r H_m^\theta - T\Delta_r S_m^\theta$ and (6), (4) about standard molar entropy of nano- Cu_2O can be replaced as

$$S_{m(\text{nano})}^\theta = S_{m(\text{bulk})}^\theta - \left[\Delta_r H_{m(\text{nano})}^\theta - \Delta_r H_{m(\text{bulk})}^\theta \right] / T + R(\ln k_{\text{nano}} - \ln k_{\text{bulk}}) \quad (8)$$

Thus, the conventional thermodynamic functions of Cu_2O nanocubes, including $\Delta_f H_{m(\text{nano})}^\theta$, $\Delta_f G_{m(\text{nano})}^\theta$, and $S_{m(\text{nano})}^\theta$ can be acquired by (3), (7) and (8), respectively.

The molar thermodynamic functions of nanomaterials are composed of two parts: the bulk phase and surface phase; while that of bulk materials is merely found in the bulk phase. Therefore, the molar surface thermodynamic functions are the difference between nano- and bulk materials.

$$G_m^s = \Delta_r G_{m(\text{nano})}^\theta - \Delta_r G_{m(\text{bulk})}^\theta \quad (9)$$

$$H_m^s = \Delta_r H_{m(\text{nano})}^\theta - \Delta_r H_{m(\text{bulk})}^\theta \quad (10)$$

However, for the relevant provisions of IUPAC, [20] the thermodynamic properties obtained during chemical reaction processes on the basis of the chemical equilibrium theory are partial molar thermodynamic properties. Therefore, the Gibbs energy obtained from transition state theory should be the partial molar surface Gibbs energy. That is, based on (6), (9) can be replaced as

$$G_{\text{Cu}_2\text{O}}^s = RT(\ln k_{\text{nano}} - \ln k_{\text{bulk}}) \quad (11)$$

For cubic nanoparticle, the theoretical formula of $G_{\text{Cu}_2\text{O}}^s$ is

$$G_{\text{Cu}_2\text{O}}^s = \left(\frac{\partial G^s}{\partial n} \right)_{T,P} = \sigma \left(\frac{\partial A}{\partial n} \right)_{T,P} = \frac{4\sigma M}{\rho l} \quad (12)$$

Although the molar surface Gibbs energy is not equal to the partial molar surface Gibbs energy, there is a clear relationship between them seen from $G_m^s = \sigma A/n = 6\sigma M/\rho l$ and (12), which is $G_{\text{Cu}_2\text{O}}^s : G_m^s = 2:3$. So the molar surface Gibbs energy of Cu_2O

nanocubes can be written as

$$G_m^s = 3/2RT(\ln k_{\text{nano}} - \ln k_{\text{bulk}}) \quad (13)$$

According to the basic equation $\Delta_r G_m^\theta = \Delta_r H_m^\theta - T\Delta_r S_m^\theta$ of thermodynamics, the molar surface entropy of Cu_2O nanocubes is

$$S_m^s = (H_m^s - G_m^s)/T \quad (14)$$

3. Experimental: The four different sizes of Cu_2O nanocubes were prepared as follows. 200 ml of deionised water and a certain concentration of trisodium citrate were mixed in a beaker, which was stirred in a water bath at 30°C for 20 min. Then, 0.5 ml of $1.2 \text{ mol} \cdot \text{l}^{-1}$ CuSO_4 was rapidly infused into the beaker. After 5 min, 0.5 ml of $4.8 \text{ mol} \cdot \text{l}^{-1}$ NaOH was dropped into the solution to react for 5 min, followed by the addition of 0.5 ml of $1.2 \text{ mol} \cdot \text{l}^{-1}$ ascorbic acid. Keeping for 30 min, orange-red precipitate was generated. The precipitate was thrice-washed through centrifugation using deionised water and absolute alcohol after standing. Finally, the precipitate was preserved in absolute alcohol by the injection of N_2 for 30 min. The average particle sizes of cubic Cu_2O prepared using trisodium citrate with concentrations of 0.3, 0.6, 0.9, and $1.2 \text{ mol} \cdot \text{l}^{-1}$ were 42, 55, 67, and 116 nm, respectively. The bulk Cu_2O and nitric acid were supplied by Aladdin Industrial Corporation and Chengdu Kelong Chemical Reagent Factory in China, separately.

The phase and purity of the as-produced Cu_2O were examined by X-ray diffraction (XRD) using an Ultima IV-type X-ray diffractometer with $\text{Cu K}\alpha$ radiation ($\lambda = 1.5406 \text{ \AA}$). The sizes, morphologies, and microstructures of Cu_2O were observed with a scanning electronic microscopy (SEM, SUPRA 55 Sapphire, Carl ZEISS) with energy-dispersive spectrometry machine (Oxford X-MaxN) attached to the instrument for detecting the compositions. The X-ray photoelectron spectroscopy (XPS) spectrum was recorded for the Cu_2O cubes using a V.G. Scientific ESCALAB MKII spectrometer with a monochromatised $\text{Al K}\alpha$ X-ray source at 1486.6 eV. The thermodynamic functions of Cu_2O nanocubes were obtained by RD 496-CK 2000 microcalorimeter from China.

Cu_2O prepared ($1.500 \pm 0.005 \text{ mg}$) with different particle sizes was weighed and placed in a sample pool of 15 ml HNO_3 solution (1.0 ml of $2.0 \text{ mol} \cdot \text{l}^{-1}$) was transferred into a small cell, which sealed together with sample pool to put into the microcalorimeter. The instrumental parameters were set and the temperature was kept at temperatures of 298.15 K. After the base line was stabilised, the small cell was pierced for mixing and reaction between Cu_2O and HNO_3 so as to obtain the in situ thermogram of the reaction process. The conventional and surface thermodynamic functions of Cu_2O with different particle sizes were calculated to acquire.

4. Results and discussion: The synthesised four different sizes of Cu_2O nanocubes are shown in Fig. 1, the corresponding average sizes of them were (a) $42 \pm 5.8 \text{ nm}$, (b) $55 \pm 6.7 \text{ nm}$, (c) $67 \pm 7.8 \text{ nm}$, and (d) $116 \pm 16.6 \text{ nm}$. The SEM images in Fig. 1 demonstrated that all the four morphologies were cube for nano- Cu_2O and their particles were uniform and concentrated. Fig. 2 showed the XRD patterns of as-synthesised Cu_2O , which indicated that all the diffraction peaks consisted with the face-centred cubic crystal systems of Cu_2O (JPCDS Card No. 05-0667). The six main diffraction peaks corresponded to crystal faces (110), (111), (200), (220), (311), and (222), separately. Furthermore, a stronger intensity of the (111) peak can be seen when compared to others and it increased with the increase of particle size. All peaks were sharp without other impurity peaks of Cu(0) and Cu(2) being found, suggested that the as-synthesised Cu_2O were not only highly crystalline but also phase pure. To further confirm the purity of the as-synthesised

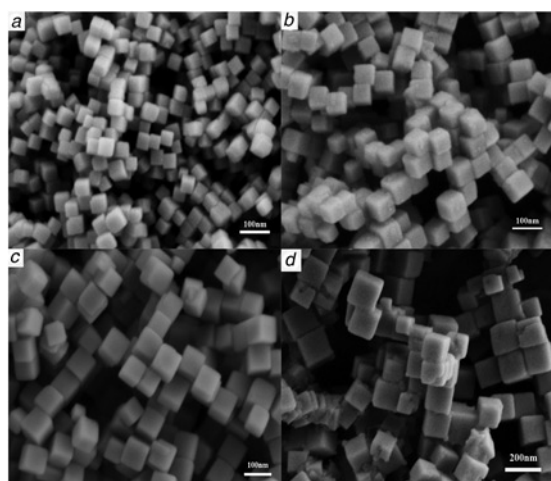


Fig. 1 SEM images of the as-produced Cu_2O nanocubes with four different particle sizes
a 42 ± 5.8 nm
b 55 ± 6.7 nm
c 67 ± 7.8 nm
d 116 ± 16.6 nm

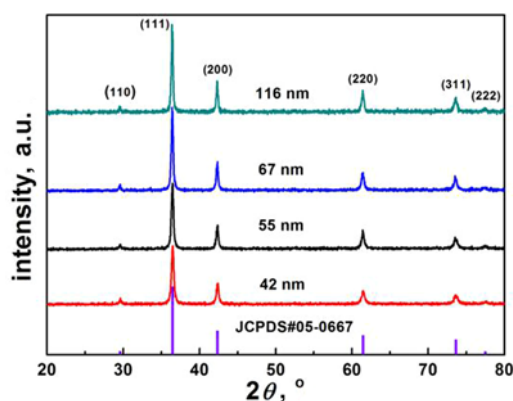


Fig. 2 XRD patterns of synthesised Cu_2O with different particle sizes
a 42 ± 5.8 nm
b 55 ± 6.7 nm
c 67 ± 7.8 nm
d 116 ± 16.6 nm

Cu_2O , the XPS was employed for obtaining the surface elemental composition and electronic state of Cu_2O . The survey spectrum of XPS, as shown in Fig. 3a, indicated that the main peaks were $\text{Cu} 2p_{3/2}$, $\text{O} 1s$, and $\text{C} 1s$ at 932.3, 530.4, and 284.8 eV, respectively. Fig. 3b showed the high-resolution spectra of $\text{Cu} 2p$ peaks, which revealed the peak at 932.3, and 952.2 eV correlated with $\text{Cu} 2p_{3/2}$ and $\text{Cu} 2p_{1/2}$ should be assigned to $\text{Cu}(1)$ [21]. While no signals associated with $\text{Cu}(0)$ or $\text{Cu}(2)$ indicated the absence of Cu , CuO , or $\text{Cu}(\text{OH})_2$ on the surface, whose binding energies of $\text{Cu} 2p_{3/2}$ corresponded to 932.6, 934.4, and 935.3 eV, [22–24] Fig. 3b demonstrated the smaller particle size, the stronger the $\text{Cu} 2p$ peak. Moreover, there was maybe 0.3 eV blue-shift of the $\text{Cu} 2p$ peak for the 116 nm Cu_2O in comparison with the 42 nm. From the results of XRD and XPS we can conclusively claim that Cu_2O is the only product, and they all exclude the existence of other species of Cu element. Therefore, the as-synthesised Cu_2O nanocubes with four different particle sizes were pure. Fig. 4 displays a typical in situ microcalorimetric heat flow curve of the reaction between Cu_2O nanocubes and HNO_3 solution. The calorimetric experiment of each reaction system was carried out 3 times, according to thermochemical cycle, the standard

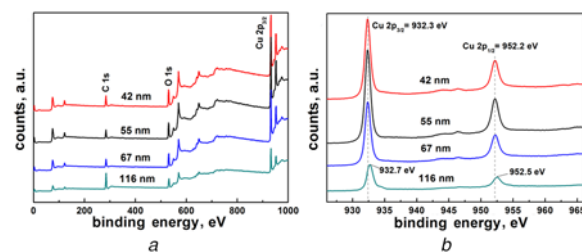


Fig. 3 XPS patterns of as-synthesised Cu_2O
a Survey spectra and
b High-resolution spectra of Cu_2O

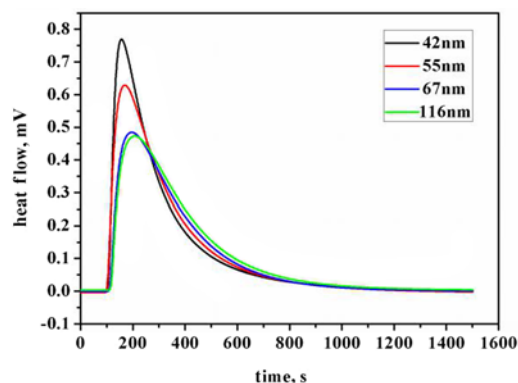


Fig. 4 In-situ microcalorimetric heat flow curve of the reaction between Cu_2O nanocubes and HNO_3 solution at temperatures of 298.15 K

Table 1 Standard molar enthalpies and rate constants of the nano Cu_2O and bulk Cu_2O reaction systems

Reaction system		$\Delta_r H_m^\theta$, $\text{KJ} \cdot \text{mol}^{-1}$	k 10^{-3} , s^{-1}
42 nm	1	−243.832	6.035
	2	−245.571	6.018
	3	−243.911	5.981
	average	-244.438 ± 0.982	6.011 ± 0.028
55 nm	1	−229.763	5.432
	2	−230.157	5.473
	3	−227.308	5.454
	average	-229.076 ± 1.554	5.453 ± 0.021
67 nm	1	−217.268	5.126
	2	−219.863	5.203
	3	−219.011	4.941
	average	-218.714 ± 1.323	5.090 ± 0.134
116 nm	1	−203.566	4.536
	2	−203.276	4.688
	3	−201.759	4.739
	average	-202.867 ± 0.97	4.654 ± 0.106
bulk	1	−175.088	3.612
	2	−176.529	3.714
	3	−175.111	3.669
	average	-175.576 ± 0.825	3.665 ± 0.051

molar enthalpies and rate constants of nano- and bulk Cu_2O with HNO_3 were obtained by carrying out linear regression on (1), and the results were shown in Table 1. Table 1 showed that the rate constant increased with the reduction of the particle size. This was because when substances were reduced to nanoscale, both the number of atoms on the surfaces and activated atoms participating in reactions increased. As a consequence, the rate constant was increased for the acceleration of the reaction rate.

Table 2 Intrinsic thermodynamic function of different sizes of Cu₂O

Intrinsic thermodynamic function	42 nm	55 nm	67 nm	116 nm
$\Delta_f G_m^\theta$, KJ · mol ⁻¹	-150.23	-149.99	-149.81	-149.59
$\Delta_f H_m^\theta$, KJ · mol ⁻¹	-99.74	-115.10	-125.46	-141.31
S_m^θ , J · mol ⁻¹ · K ⁻¹	93.34	93.28	93.25	93.19
G_m^s , KJ · mol ⁻¹	1.226	0.985	0.814	0.592
H_m^s , KJ · mol ⁻¹	68.862	53.500	43.138	27.291
S_m^s , J · mol ⁻¹ · K ⁻¹	226.85	176.14	141.95	89.55

The values of $\Delta_f G_m^\theta$, $\Delta_f H_m^\theta$, and S_m^θ of bulk Cu₂O at 298.15 K were referred to be -149.0, -168.6, and 93.1 J · mol⁻¹ · K⁻¹ separately from Lange's Handbook of Chemistry [25]. While the values of $\Delta_f G_m^\theta$, $\Delta_f H_m^\theta$, and S_m^θ of Cu₂O nanocubes were calculated by (7), (3), and (8). On the basis of the data of the reaction rate constants and reaction enthalpies from Table 1, the molar surface Gibbs energy, the molar surface enthalpy, and the molar surface entropy were calculated by (13), (10), and (14), respectively.

The corresponding data are shown in Table 2. Table 2 showed that, $\Delta_f H_m^\theta$ and S_m^θ tend to increase while $\Delta_f G_m^\theta$ tends to decrease with the decrease in particle size. Apparently, $\Delta_f G_m^\theta$, $\Delta_f H_m^\theta$, and S_m^θ of Cu₂O nanocubes were all greater than those of bulk Cu₂O. Since particle size of Cu₂O decreased to nanoscale, activated atoms on the surface phase increased and participated the reaction, which led to a large amount of heat being released and the degree of disorder being increased. Therefore, $\Delta_f H_m^\theta$ and S_m^θ of Cu₂O nanocubes were increased. It can be explained from (1) that the increase of the rate constant had resulted in the decrease of $\Delta_f G_m^\theta$ of Cu₂O nanocubes with decreasing particle size. At the same time, the G_m^s , H_m^s , and S_m^s of Cu₂O nanocubes all increased with decreasing particle size. This is not only in line with the models of the molar surface thermodynamic functions built in $G_m^s = \sigma A/n = 6\sigma M/\rho l$ to $S_m^s = -6M/\rho l[(\partial\sigma/\partial T)_p + (2/3)\sigma\alpha]$, but also due to the increase of the number of surface atoms as substances were ultra-fined to the nanoscale. Those atoms with uneven stress and dangling bonds can cause the enhancement of surface adsorption and activation capacities, the increasement of the potential of the surface phased and addition to the disordered of the surface atoms. Therefore, G_m^s , H_m^s , and S_m^s all increased with decreasing particle size. According to the theories of reaction kinetics, the rising temperature accelerates the thermal motion of particles, and increases the vibration frequency of surface atoms, which led to increase in both the kinetic energy and internal energy of the electrons. Based on the classic theory of heat capacity, when substances were reduced to nanoscale, the density and the average energy needed for the variation of surface atoms increased. This is why G_m^s , H_m^s , and S_m^s all increased with decreasing particle size.

5. Conclusion: In summary, four different sizes of Cu₂O nanocubes were synthesised by liquid phase reduction method. The conventional and surface thermodynamical functions of Cu₂O nanocubes were obtained on the basis of thermo-chemical cycles and transition state theory. The effect of particle size on conventional thermodynamic functions as well as surface thermodynamic functions were investigated. The results suggest that the conventional thermodynamical functions of Cu₂O nanocubes, like $\Delta_f H_m^\theta$ and S_m^θ , increased with the reduction of particle size, while $\Delta_f G_m^\theta$ decreased. Moreover, the surface thermodynamic functions of Cu₂O nanocubes, including G_m^s , H_m^s , and S_m^s increased with the reduction of particle size. It is of great significance and value for studying surface physicochemical of solid materials. Besides, this research provides a novel method for the acquisition of

thermodynamical functions of nanomaterials and the investigation of particle size thereon.

6. Acknowledgments: This work was supported by the National Natural Science Foundation of China (grant nos. 21273050, 21573048, 201873022), and the Innovation Project of Guangxi University for Nationalities Graduate Education (grant no. gxun-chxzs2016120).

7 References

- [1] Zhang L.D.: 'Nanomaterials and nanostructures' (Science Press, People's Republic of China, 2011)
- [2] Wen Y.Z.: 'Thermodynamics of nanoadsorption from solution: theoretical and experimental research', *J. Chem. Thermodyn.*, 2015, **80**, pp. 112–118
- [3] Xu L.: 'Comparison study on the stability of copper nanowires and their oxidation kinetics in gas and liquid', *ACS Nano*, 2016, **10**, pp. 3823–3834
- [4] Tan C.S.: 'Facet-dependent electrical conductivity properties of Cu₂O crystals', *Nano Lett.*, 2015, **15**, pp. 2155–2160
- [5] Pang H.: 'Morphology effect on antibacterial activity of cuprous oxide', *Chem. Commun.*, 2009, **9**, pp. 1076–1078
- [6] Chakravarty A.: 'Cu₂O nanoparticles anchored on amine-functionalized graphite nanosheet: a potential reusable catalyst', *Langmuir*, 2018, **31**, pp. 5210–5219
- [7] Zhang X.R.: 'Rapid spectrophotometric method for determining surface free energy of microalgal cells', *Anal. Chem.*, 2014, **86**, pp. 8751–8756
- [8] Nguyen M.A.: 'Direct synthetic control over the size, composition, and photocatalytic activity of octahedral copper oxide materials: correlation between surface structure and catalytic functionality', *ACS Appl. Mater. Interfaces*, 2015, **7**, pp. 13238–13250
- [9] Kuang Q.: 'High-energy-surface engineered metal oxide micro- and nanocrystallites and their applications', *Acc. Chem. Res.*, 2013, **47**, pp. 308–318
- [10] Freakley S.J.: 'Palladium-tin catalysts for the direct synthesis of H₂O₂ with high selectivity', *Science*, 2016, **351**, pp. 965–968
- [11] Jamshidian M.: 'A continuum state variable theory to model the size-dependent surface energy of nanostructures', *Phys. Chem. Chem. Phys.*, 2015, **17**, pp. 25494–25498
- [12] Range S.: 'Size matters: an Experimental and computational study of the influence of particle size on the lattice energy of NaCl', *J. Phys. Chem. C*, 2015, **119**, pp. 4387–4396
- [13] Navrotsky A.: 'Nanophase transition metal oxides show large thermodynamically driven shifts in oxidation-reduction equilibria', *Science*, 2010, **330**, pp. 199–201
- [14] Hayun S.: 'Nanoceramics – Energetics of surfaces, interfaces and water adsorption', *J. Am. Ceram. Soc.*, 2011, **94**, pp. 3992–3999
- [15] Zeng X.C.: 'Theory and method of chemical reaction thermodynamics' (Chemical Industry Press, Beijing, 2003)
- [16] Fan G.C.: 'Size effect on thermodynamic properties of CaMoO₄ micro/nano materials and reaction systems', *Solid State Sci.*, 2013, **16**, pp. 121–124
- [17] Li X.X.: 'Size effects on reaction kinetics and surface thermodynamic properties of nano-octahedral cadmium molybdate', *Chin. Sci. Bull.*, 2014, **59**, pp. 2490–2498
- [18] Gao S.L.: 'Derivation and application of thermodynamic equations', *Chin. J. Inorg. Chem.*, 2002, **18**, pp. 362–366
- [19] Fu X.C.: 'Physical chemistry 5th edn' (Higher Education Press, People's Republic of China, 2006), pp. 235–344
- [20] Cohen E.R.: 'Quantities, units and symbols in physical chemistry 3rd edn' (Royal Society of Chemistry, UK, 2007)
- [21] Barreca D.: 'CVD Cu₂O and CuO nanosystems characterized by XPS', *Surf. Sci. Spectra*, 2007, **14**, pp. 41–51
- [22] Tahir D.: 'Electronic and optical properties of Cu, CuO and Cu₂O studied by electron spectroscopy', *J. Phys.: Condens. Matter*, 2012, **24**, p. 175002
- [23] Yang Y.: 'Controllable morphology and conductivity of electro-deposited Cu₂O thin film: effect of surfactants', *ACS Appl. Mater. Interfaces*, 2014, **6**, pp. 22534–22543
- [24] Lefevre G.: 'Sorption of iodide on cuprite Cu₂O', *Langmuir*, 2000, **16**, pp. 4519–4527
- [25] Dean J.A.: 'Lange's handbook of chemistry 15th edn' (McGraw-Hill, USA, 1998), pp. 6–103